LLNL-TR-752770

LAWRENCE
LIVERMORE
NATIONAL
LABORATORY

Optimization of PDMS Photoresin for Three-Dimensional Printng via Projection Micro-Stereolithography

S. Ruelas

June 11, 2018

Disclaimer

This work performed under the auspices of the U.S. Department of Energy by Lawrence Livermore National Laboratory under Contract DE-AC52-07NA27344.

Optimization of PDMS photoresin for 3D-prinitng via projection micro-stereolithography

Samantha Ruelas
Lawrence Livermore National Laboratory*
LLNL-TR-752770

Abstract

As an industry, additive manufacturing (AM) has provided a way to quickly build structures in a cost-effective manner. Furthermore, the ability to utilize a computer aided design file to build said structures permits rapid customization of parts. Three-dimensional (3D) printing, specifically projection micro-stereolithography (PµSL), has these qualities in addition to not being restricted by a structure's geometry. However, printing using a PµSL system is limited by the chemistry the resin undergoes and by resin viscosity. In this work, silicone structures were printed via a thiol-ene "click" reaction, which is less sensitive to oxygen inhibition compared to commercial resins. The resin chemistry was optimized in order to decrease feature size. Formulation changes along with various light intensity doses and exposure times resulted in a 50% decrease in feature sizes. Silica filler was added to the resin to increase mechanical strength. A post-cure procedure did not improve the material's strength, suggesting a full cure is reached during printing.

*This work was performed under the auspices of the U.S. Department of Energy by Lawrence Livermore National Laboratory under Contract DE-AC52-07NA27344.

Introduction

The field of additive manufacturing has expanded and merged chemistry and engineering due to the advancement of printing technology and the expanding pool of materials used. 3D printing of materials is used in various fields such as the biomedical, electronics, and even construction industry.[1] This is because it has the ability to customize structures quickly and produce small quantities at a lesser cost. 3D printing offers a way to rapidly build a structure by cutting it into multiple 2D layers and piecing them together using computer aided design (CAD).[2] More specifically, PμSL uses a stereolithography file (STL) to cut the structure into thin layers. The STL controls the structure's geometry for each layer, layer thickness, and resolution.[2] Printing via PμSL provides the ability to print complex geometries with voids and curvatures, in addition to being able to quickly modify a structure by changing the digital STL. These elements are highly sought-after when considering other forms of lithography, such as x-ray, photolithography, and soft lithography.[3, 4, 5] These techniques are expensive due to the masks required to project images, they require multiple processes which are time consuming, and restrict geometry because curves cannot be formed.

Silicone is an example of an elastomer that is used in applications such as biomedical devices, wearable electronics, and bioreactors. It is gas-permeable, water-impermeable, inert, and translucent, making it an ideal material to be able to print. Moreover, printing materials that are less glassy and brittle can open doors to different industries. Currently, silicone structures are generally shaped by injection molding, hindering the geometry that can be manufactured.[6,7] Here, we discuss the printability of silicones via UV-initiated thiol-ene click chemistry using PμSL. Click reactions are known to produce high yields, be versatile, and selective—three factors that are ideal in a chemical reaction. A major driving force for the use of thiol-ene click reactions is their ability to proceed at room temperature in the presence of oxygen, without hazardous amounts of solvent or pressure.[8] **Equation 1** depicts the reaction that occurs between monomers to form a crosslinked network with a PDMS backbone. It is known that PDMS functions as a poor solvent, which was observed when testing the solubility of thiol chains and reagents.[9]

Equation 1. A photoinitiated click reaction between the thiol groups and the vinyl takes place in ambient conditions to form a crosslinked polymer with a siloxane backbone.

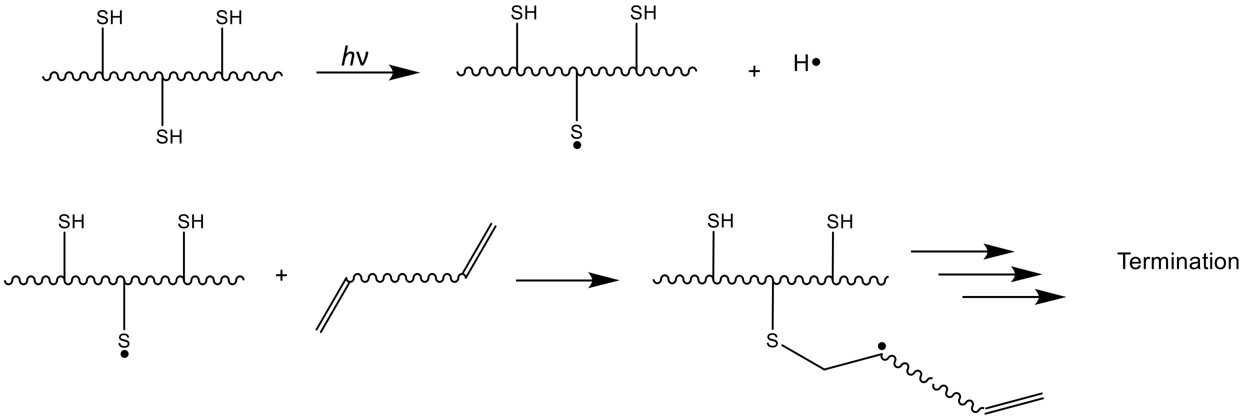

Another challenge was printing silicone resins with certain viscosities. Our PμSL paste system, Mark IV, starts with lowering a build plate to the floor of the photocurable resin pool. The acrylic resin pool floor ensures a thin layer of resin will be in contact with the build plate by squeezing out excess resin. An image is projected into the resin pool with a predetermined intensity and exposure time. The polymerization occurs, and a layer of solid material is left on the build plate. The build plate is raised, the stage rotates, as the stage rotates a wiper blade spreads resin, and the process is repeated. **Figure 1** shows the general setup. This “stamping” mechanism allows the printing of paste-like resins, which other systems cannot do. Moreover, Mark IV has a larger print area compared to other inhouse PμSL systems. The x and y dimension, or length and width, are controlled by the build plate dimensions. The z-direction is determined by how high the build plate can move. Currently a build area of 3.5 cm x 3.0 cm x 12.0 cm can be achieved. These larger structures can be built in less time depending on layer thickness; however, there is a resolution trade off that correlates with a larger build area, increased speed, and viscous resins.

Figure 1. The PμSL paste system, Mark IV, was made inhouse. There is a projector with a 405 nm LED light source that transmits the image to the bottom of rotating stage containing photoresin. The polymerization occurs between the floor of the stage and the build plate. The cured resin adheres to the build plate, the stage rotates, and the process is repeated until the entire structure has been printed.

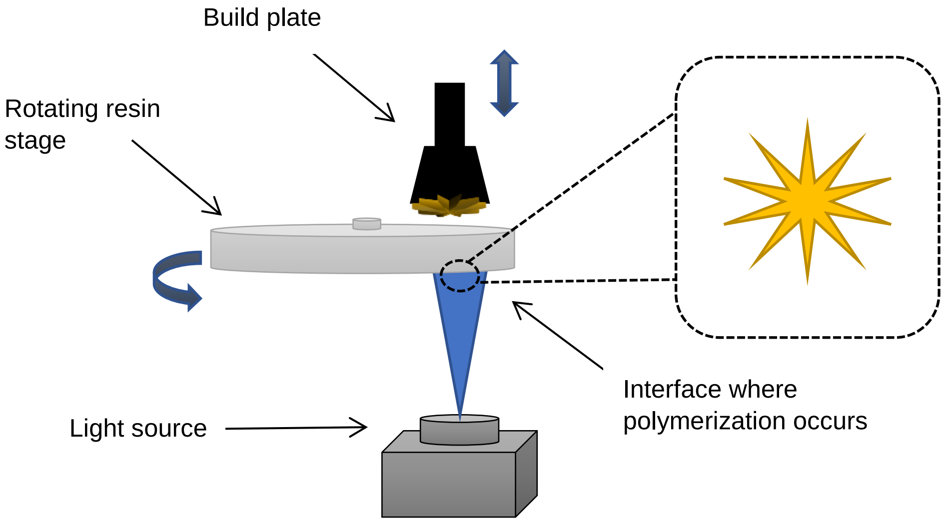

Experimental

Materials. Both monomers and silicon dioxide filler were purchased from Gelest Inc. Isopropylthioxanthone (ITX), 2,5-Bis(5-*tert*-butyl-benzoxazol-2-yl)thiophene (BBOT), 4-methoxyphenyl (MEHQ), 2-ethylhexyl 4-(dimethylamino)benzoate (EHDA), 2-(2H-benzotriazol-2-yl)-4,6-di-tert-pentylphenol (BTA) , and tetrahydrofuran (THF) were purchased from Sigma Aldrich. Genocure TPO-L (TPO-L) was purchased from Lambson.

PµSL Mark IV. The printer was equipped with a DLi 6500 Projector, which emits light at 405 nm. The optical design was preformed onsite. Printer accessories such as resin stage and wiper were printed onsite. Light intensity experiments were performed with an optical power meter from Thorlabs showing 45 mW of power projected. From now on light intensity is reported as a percentage of 45 mW.

Silicone resins. A 4.2:1 ratio of DMS-V31:SMS-042 was used in all resin formulations. DMS-V31 functioned as the vinyl component and SMS-042 provided thiol groups. When filler was used, silica was added by wt. % to the resin mixture. The silica was added a few grams at a time and mixed in with a spatula to avoid agglomeration of silica. The mixture was then mixed with a Thinky Planetary Centrifugal Mixer for 3-5 minutes, depending on silica content, to form a homogeneous resin.

Photoinitiator, photoabsorber, and inhibitor were added according to wt. % of monomers added in the resin mixture, not monomer weight and filler weight (**Table 1**). Each reagent was weighed out separately, dissolved in minimal THF, then added to the resin mixture. The reagents were then manually stirred into resin with a spatula until the yellow coloring from the ITX faded. The resin was stirred with a Thinky mixer for another 3 minutes.

Table 1. Photoinitiator, photoabsorber, and inhibitor were added to resin mixture according to total amount of monomer present. They were then dissolved individually in THF and added to the resin mixture. A Thinky mixer was used to ensure a homogenous resin.

Photoinitiator	Photoabsorber	Inhibitor
ITX (0.3 wt. %) EHDA (0.6 wt. %)	BBOT (0.12 wt. %)	MEHQ (0.05 wt. %)

Tensile Testing. Dog bones about 1.0 mm thick were printed using the formulation mentioned in Table 1. A post cure procedure consisting of a 30 s UV exposure on both sides of the dog bone was performed for each sample except for a secondary batch of dog bones with 25% filler. A dynamic tensile test was conducted with an Instron 5943. Samples were stretched at a rate of 0.25 mm/s.

Feature Measurements. A one-layer sample of the resin was collected by removing the build stage from the printer. The STL was projected for the set exposure time, the run was cancelled and a one-layer structure was produced without interference from the build plate in the z-dimension. The sample was removed from the resin stage with tweezers and placed on a sheet of McMaster-Carr rubber. All measurements were conducted with resin containing 10% filler to reduce damage during removal process. The sample features were then measured in the x, y, and z-dimensions using a Zeiss Stereo Discovery.V12 microscope. A minimum of three separate measurements for each individual feature were averaged—all reported measurement values are averages.

Solubility Tests. Both vinyl and thiol monomers were mixed in the corresponding ratio. No filler was added to keep the resin clear and colorless. Vials with 3.0 g of monomer mixture were set up. One reagent was added to each vial with a concentration 4 times higher than what is typically used. Five 2-fold serial dilutions were performed or until the reagent no longer crashed out of solution. The vials were left in ambient conditions for a 45-day period. The concentrations reported were still in solution after 45 days.

Initiator Degradation. When printed structures were left in ambient light, a yellowing of the material occurred over time. To check if the initiator caused the yellowing, ITX was added to an aliquot of DMS-V31 and SMS-042. A bulk tab was cured with a UV box. The same was done with TPO-L as the initiator. Both samples were left in direct sunlight. The sample containing ITX yellowed after 7 days, the TPO-L sample remained clear and colorless after 21 days in the sun.

Results and Discussion

A baseline of the current resin was needed in order to pinpoint areas requiring improvement. A one-layer structure programed with feature sizes from 100 μm to 2000 μm was printed (**SI Figure 1**). The structures were printed with different combinations of intensities (40, 50, 70, 80, and 100%), and exposure times (5, 7 and 10 seconds). Smaller feature sizes were not resolved due to optical limitations. The features that were resolved had increased feature sizes correlating with increased intensity and exposure time (**Figure 2**). An intensity of 50% for 7 seconds appeared to produce the most accurate feature sizes at 500 µm.

Layer thickness was also examined, and they were found to be up to 500 µm thick. Given that layers are programed to be 30-50 µm thick, having a polymerization depth of 500 µm causes a distortion in structures. Structure layers bleed into the subsequent layers and gaps within structures are filled. This is apparent in the printed log pile structure in **Figure 3**. The red scale bars show where the layer should stop, but the vertical pillars bled into the horizontal layers. The image on the lower right is a snap shot of the STL used, and illustrates how the structure should appear in the absence of overpolymerization.

Figure 2. The STL used to find the limitations of the resin had lines of varying widths from 100 to 2000 μm. The difference between the programed feature size and the printed feature size aided in in determining overpolymerization in the x and y dimensions was

occurring. An intensity of 50% at 7 seconds produced the best feature size, but further formulation changes were needed to decrease feature sizes.

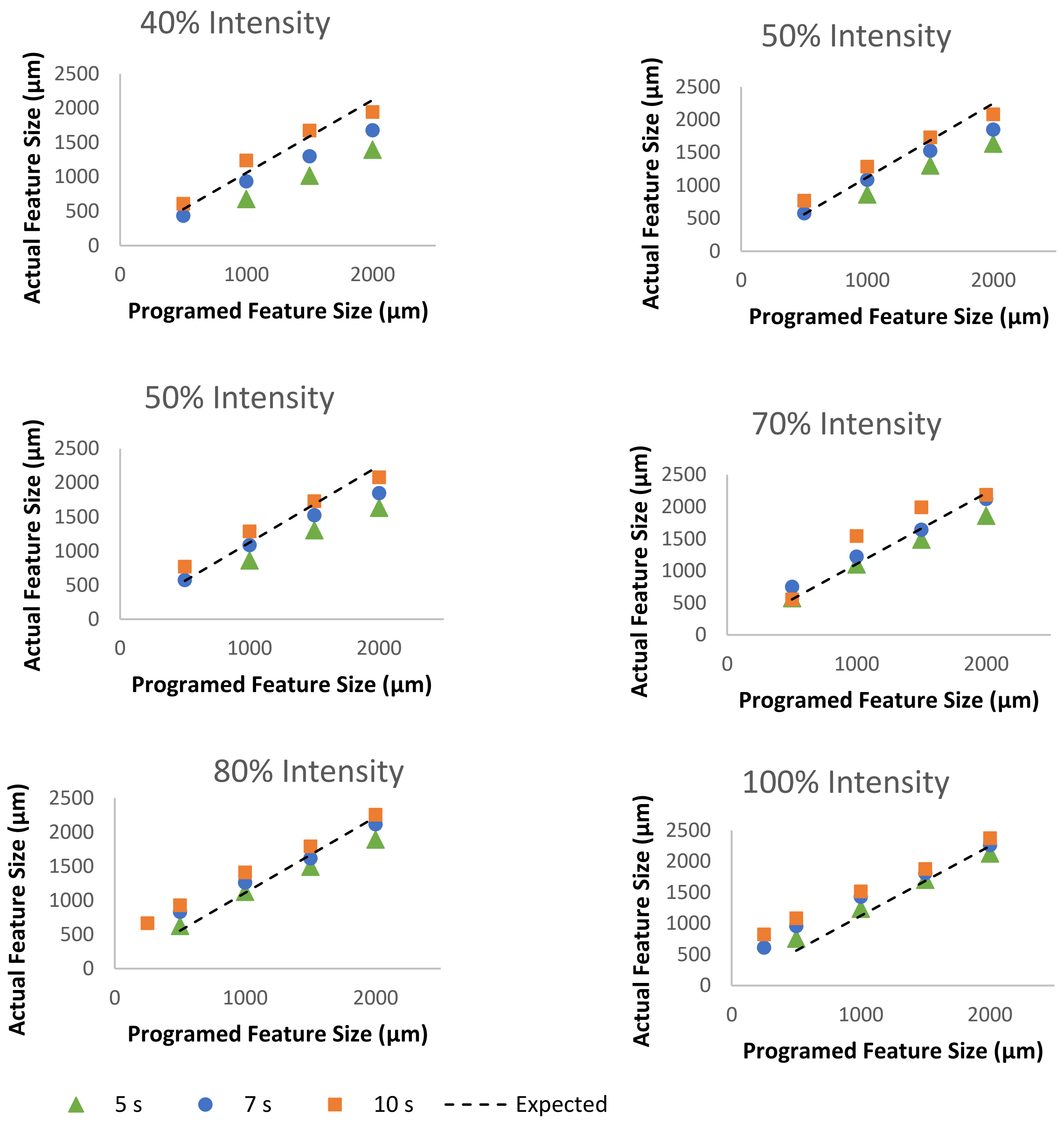

Figure 3. The image on the lower right shows what the log pile structure is programed to look like. The image on the upper right shows how the structure prints. The red scale bars depict the dimensions that were expected. A 1 mm gap between pillars was observed, meaning 0.5 mm pillar thickness was achieved and no overpolymerization in the x-direction occurred. On the other hand, overpolymerization in the z-direction was seen bleeding into the horizontal layer below.

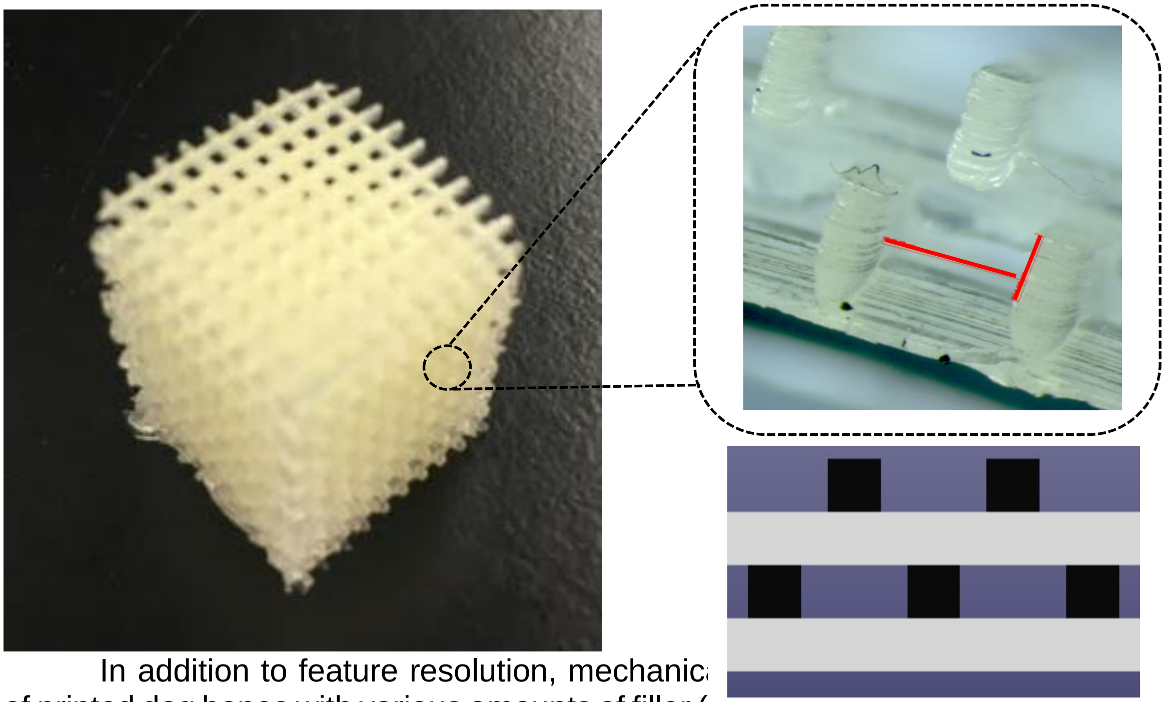

In addition to feature resolution, mechanic esting of printed dog bones with various amounts of filler (ducted using an Instron. A linear relationship between amount of filler and elongation of the sample was observed, supporting the notion that increased filler reinforces mechanical strength (**Figure 4**). Unfortunately, with increased filler content comes increased viscosity. Although Mark IV was made to print resins with higher viscosities, resins that do not flow have a decreased printability.[11] As the building plate comes down to meet the resin stage and the excess resin flows away from the building plate and air bubbles are pushed out. A gel-like resin does not flow away from the building stage as well and air bubbles are trapped within the printed layer; therefore, causing thicker layers and voids in the structure. These voids can hinder the strength of a structure. Tensile testing of another batch of samples with 25% filler was conducted, but they did not undergo the post-cure procedure. A smaller elongation was expected, but a slightly higher elongation compared to the post-cured samples was observed. This data suggests that structures reach their conversion limit of monomer to polymer during the printing process.

Figure 4. Mechanical strength testing was conducted via Instron tensile testing. The printed dog bones with various filler amounts display a linear relationship between amount of filler in the material and the elongation it can undergo before failure. The samples that were not post cured preformed slightly better than their post-cured counterparts, suggesting a full cure was achieved during the printing process.

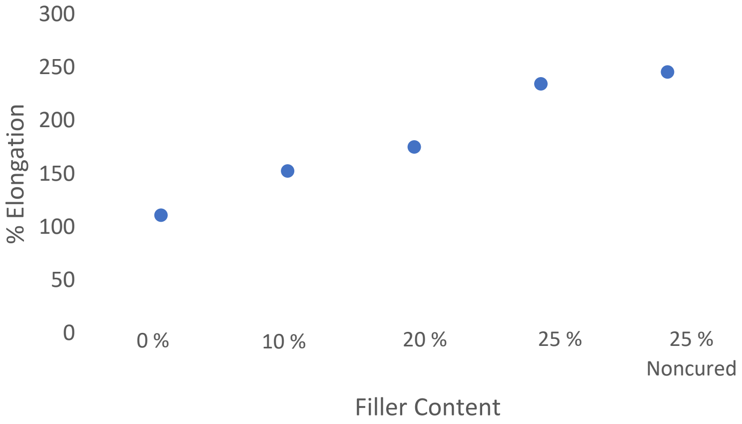

In order to further optimize feature size, a solubility screening of initiator, absorber, and inhibitor in the resin mixture was carried out (**Table 2**). Some ITX cashed out at 0.3 wt. %, but reducing the concentration to 0.15 wt. % kept all the initiator in solution. BBOT crashed out at larger amounts than expected—7 2-fold dilutions were preformed to keep the photoabsorber in solution, bringing the concentration to 0.003 wt. %. Another photoabsorber, BTA, underwent the same solubility test, and stayed in solution at 0.24 wt. %. In addition, a Type I initiator, TPO-L, had a maximum solubility of 0.06 wt. %. With the given solubility results, the photoabsorber was changed to BTA, but ITX was kept as the photoinitiator.

Table 2. Reagent solubility issues within the resin are not surprising as silicones are incompatible with molecules containing small amounts of hydrocarbons. The last column shows the maximum amount of reagent that can be added to the resin before it begins to fall out of solution. ITX had slight solubility issues in the resin, but reducing the amount to 0.15 wt. % ensured solubility. The photoabsorber used was changed from BBOT to BTA due to BTA's silicone-soluble properties.

Reagent	Wt. % used	Maximum wt. %
ITX/EHDA	0.30/0.60	0.15/2.40
BBOT	0.12	0.003
MEHQ	0.05	0.20
BTA	---	0.24
TPO-L	---	0.06

The solubility issues associated with BBOT meant, structures were being printed without virtually any photoabsorber present. This is reinforced by the overpolymerization seen in **Figure 3**. In an effort to combat the large cure depth, BTA was used at 0.48, 0.24, 0.12, and 0.06 wt. %. At a 50 % intensity for 7 seconds, the combination of ITX and BBOT produced 500 μm features when it was programed to. To check if BTA performed better, 500 μm features were programed with 1000 μm supports on the side (**SI Figure 2**). The samples were printed at a 60% intensity for 7 seconds to ensure curing. For all samples containing BTA, a feature size of about 325 μm was observed despite the expected 500 μm size (**Figure 5**). A trend between higher concentrations of BTA and smaller feature sizes is not observed. This could be due to damage undergone as the sample is removed from the rotating stage or a larger sample pool is needed to verify the values observed. A dip in the graph is consistent for all samples, indicating smaller features in that region. This data point corresponds to the largest spacing between features, 2000 µm, which has sharper lines because the blending of neighboring features is not possible at that distance. The thickness of the layers was also measured to be about 250 µm, a decrease of about 50% compared to BBOT.

Figure 5. Feature sizes produced by various concentrations of BTA were measured to be about 325 µm when 500 µm was programed. The difference in sizes shows how the chemistry is being inhibited by higher concentrations of BTA in the resin compared to BBOT.

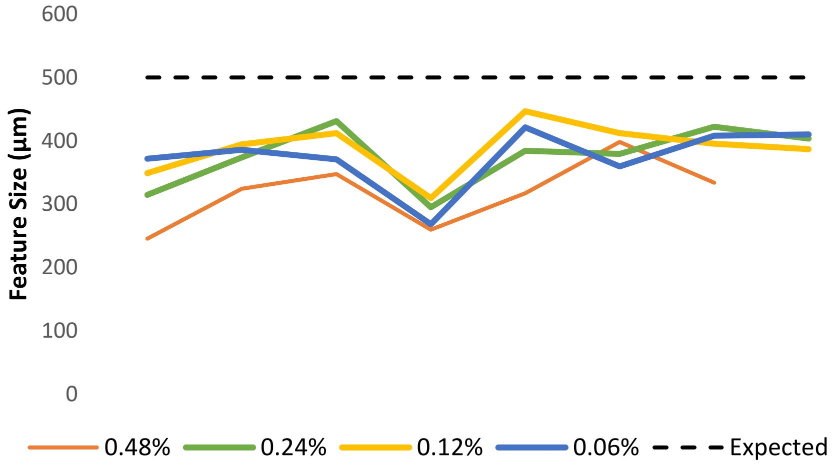

In addition to changing the photoabsorber, a new photoinitiator was tested. ITX has the coveted property of being silicone-soluble, but it yellows over time. **Figure 6** shows a freshly printed layer on the left and a printed layer that had been exposed to ambient light. The color difference is obvious and currently only a cosmetic problem. Degradation studies over time are of interest in the future, and a photoinitiator that works as well as ITX without the yellowing is currently being screened. TPO-L appears to cure just as fast as ITX in a bulk setting, but experiments are being conducted to test curing rate with the same light intensity that Mark IV produces. Unfortunately, TPO-L is less soluble than ITX as seen in the solubility experiments in **Table 2**.

Figure 6. The newly printed layer on the left is clear and colorless, while the layer on the right yellowed after being exposed to ambient light. Photoinitiator screenings were conducted to replace ITX due to yellowing observed over time.

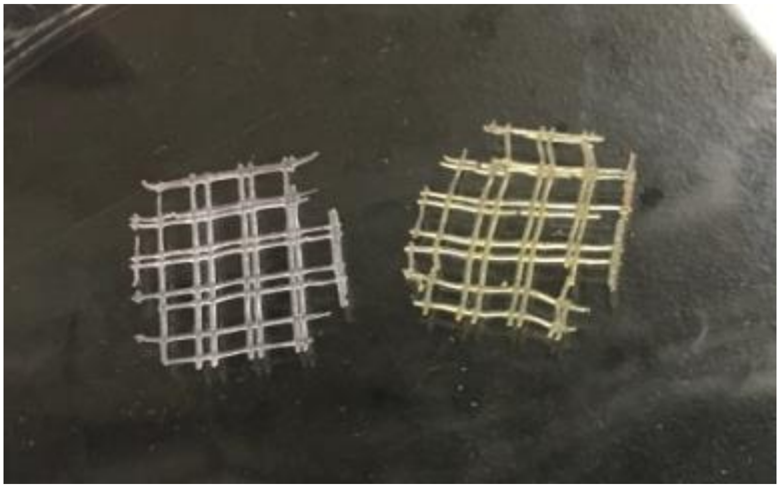

Conclusion

Here we report the ability to print silicone structures via a photoinitiated click reaction using thiol and vinyl monomers. A baseline of the current resin being printed was performed to evaluate needed improvements. The printing and measuring of structure features shows a clear trend between increased light dosages and increased feature sizes. Moreover, a light intensity of 50% for 7 seconds produced 500 μm features--the smallest observed consistently. Tensile testing of the formulation with increasing amounts of filler were carried out. As filler content was increased, an increase in mechanical strength was observed. Samples used for tensile testing were subjected to more light exposure to complete any curing of leftover monomer in the structure. A non-treated sample performed better than samples that underwent the post-cure procedure. This is evidence that the resin reaches a full cure during the printing process.

To further improve feature size, a solubility study of the reagents used was conducted. The photoabsorber used was barely soluble in the silicone resin, but BTA was 80 times more soluble than BBOT. Features programed to be 500 μm came out to be an average of 325 μm using BTA instead of BBOT—the smallest observed using Mark IV. However, layer thickness appeared to be impacted largely by light intensity rather than amount of photoabsorber present.

In the future, photoinitiators that cure as well as ITX, but do not cause yellowing of the material will be screened. Measurements of feature sizes will be performed in triplicate to better understand the error bars associated with printing such small features. Most importantly, the resolution of projected images will be optimized to aid in decreasing feature sizes.

References

1. Berman, B. 3-D printing: The new industrial revolution, Business Horizons, 55(2), 155-162 (**2012**).
2. Wong, K. V and Hernandez, A. A Review of Additive Manufacturing. *ISRN Mechanical Engineering*, Vol 2012 (**2012**).
3. Noorani, R. Rapid Prototyping—Principles and Applications, John Wiley & Sons (**2006**).

4. Hersener, J.; Piper, E.; Eilhelm, A. and Birkenstock, G. *J. Vac Sci. Technol. B*. 5(1), 253-256 (**1987**).
5. van Santen, H. and Neijzen, J. H. A. *Opt. Microlithography Sci.*, 5040, 1750-1755 (**2003**).
6. Qin, D.; Xia, Y.; and Whitesides, G. M. *Nature Protocols*, 5(3), 491-502 (**2010**).
7. Rolland, J. P.; Van Dam, R. M.; Schorzman, D. A.; Quake, S. R.; and DeSimone, J. M. *J. Am. Chem. Soc.*, 126(8), 2322-2323 (**2004**).
8. Rogers, J. A.; and Nuzzo, R. G. *Mater. Today*, 8, 50-56 (**2005**).
9. Uygun, M.; Tasdelen, M. A.; and Yagci, Y. *Macromol. Chem. Phys*. 211, 103-110 (**2010**).
10. Lee, J. N.; Park, C.; and Whitesides, G. M. *Anal. Chem.*, 75, 6544-6554 (**2003**).
11. Durban, M. M; Lenhardt, J. M.; Wu, A. S; Small, W.; Bryson, T. M.; Perez-Perez, L.; Nguyen, D. T.; Gammon, S.; Smay, J. E.; Duoss, E. B.; Lewicki, J. P.; and Wilson, T. S. *Macromol. Rapid Commun*. (**2017**).

Supporting Information

Figure 1. The STL was used to determine how well the projected image features coincided with the actual printed structures. The smallest feature consistently resolved was 500 μm, at an intensity of 50% with an exposure time of 7 seconds.

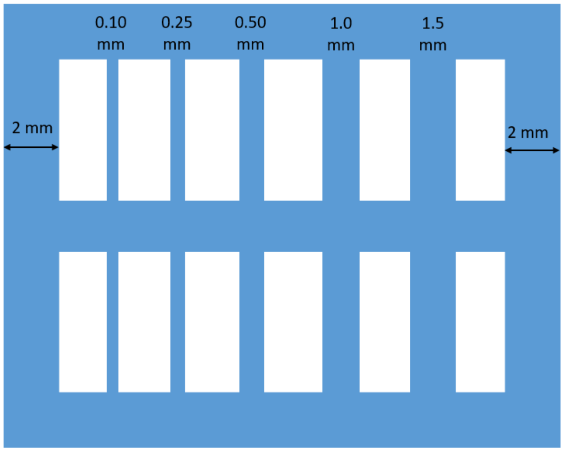

Figure 2. In order to gauge if BTA was a better photoabsorber than BBOT, an STL with 500 μm features and 1000 μm supports was programed. A decrease in feature size was observed with BTA.

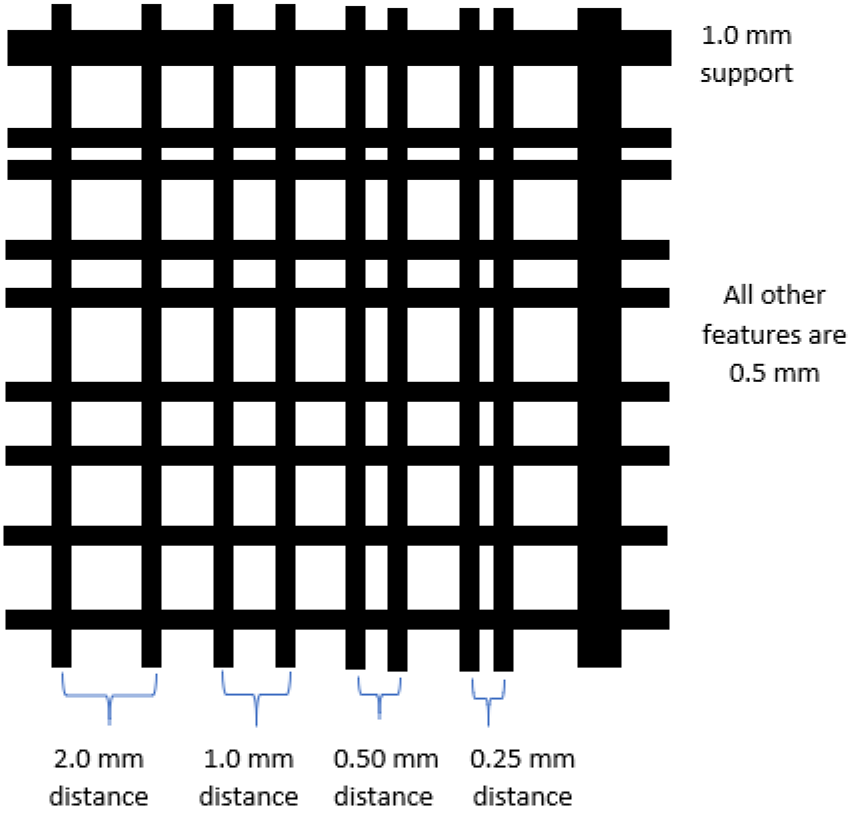
1.0 mm
support
All other
features are
0.5 mm
2.0 mm
distance
1.0 mm
distance
0.50 mm
distance
0.25 mm
distance